Available online at www.sciencedirect.com
ScienceDirect
Journal of Inorganic Biochemistry 102 (2008) 1397–1405
Journal of Inorganic Biochemistry
www.elsevier.com/locate/jinorgbio

Diorganotin(IV) complexes of dipeptides containing the α-aminoisobutyryl residue (Aib): Preparation, structural characterization, antibacterial and antiproliferative activities of $[(n\text{-Bu})_2\text{Sn}(\text{H}_{-1}\text{L})]$ (LH = H-Aib-L-Leu-OH, H-Aib-L-Ala-OH)

Eugenia Katsoulakou [a], Manolis Tiliakos [a,b], Giannis Papaefstathiou [c], Aris Terzis [d], Catherine Raptopoulou [d], George Geromichalos [e], Konstantinos Papazisis [f], Rigini Papi [g], Anastasia Pantazaki [g], Dimitris Kyriakidis [g], Paul Cordopatis [b], Evy Manessi-Zoupa [a,*]

[a] Department of Chemistry, University of Patras, 265 04 Patras, Greece
[b] Department of Pharmacy, University of Patras, 265 04 Patras, Greece
[c] Department of Chemistry, University of Athens, 157 71 Athens, Greece
[d] Institute of Materials Science, NCSR "Demokritos", 153 10 Aghia Paraskevi Attikis, Greece
[e] Symeonidio Research Center, Theagenion Cancer Hospital, 540 07 Thessaloniki, Greece
[f] 3rd Department of Clinical Oncology, Theagenion Cancer Hospital, 540 07 Thessaloniki, Greece
[g] Department of Chemistry, Aristotle University of Thessaloniki, 541 24 Thessaloniki, Greece

Received 23 May 2007; received in revised form 28 December 2007; accepted 2 January 2008
Available online 8 January 2008

Abstract

Two new organotin(IV) complexes with dianionic dipeptides containing the α-aminoisobutyryl residue (Aib) as ligands are described. The solid complexes $[(n\text{-Bu})_2\text{Sn}(\text{H}_{-1}\text{L}_\text{A})] \cdot 2\text{MeOH}$ (**1** · 2MeOH) ($\text{L}_\text{A}\text{H}$ = H-Aib-L-Leu-OH) and $[(n\text{-Bu})_2\text{Sn}(\text{H}_{-1}\text{L}_\text{B})] \cdot \text{MeOH}$ (**2** · MeOH) ($\text{L}_\text{B}\text{H}$ = H-Aib-L-Ala-OH) have been isolated and characterized by single-crystal X-ray crystallography and spectroscopic techniques ($\text{H}_{-1}\text{L}^{2-}$ is the dianionic form of the corresponding dipeptide). Complexes **1** · 2MeOH and **2** · MeOH are monomeric with similar molecular structures. The doubly deprotonated dipeptide behaves as a N(amino), N(peptide), O(carboxylate) ligand and binds to the Sn^{IV} atom. The five-coordinate metal ion has a distorted trigonal bipyramidal geometry. A different network of intermolecular hydrogen bonds in each compound results in very dissimilar supramolecular features. The IR, far-IR, Raman and ^{119}Sn NMR data are discussed in terms of the nature of bonding and known structures. The antibacterial and antiproliferative activities as well as the effect of the new compounds on pDNA were examined. Complexes **1** and **2** are active against the gram-positive bacteria *Bacillus subtilis* and *Bacillus cereus*. The IC_{50} values reveal that the two compounds express promising cytotoxic activity *in vitro* against a series of cell lines.

Keywords: α-Aminoisobutyric residue (Aib); Antiproliferative and antibacterial activity; Diorganotin(IV) complexes; Dipeptide complexes; X-ray crystal structures

1. Introduction

Nowadays, it is well known that organotin compounds of the general formula $\text{R}_n\text{SnX}_{4-n}$ exhibit a variety of biological effects depending on the number n, on the type of the organic group R bound to the metal ion and on the ligand X^- [1]. This activity ranges from severe toxicity [2] to potential pharmacological applications. The most extensively studied field of these applications is based on the findings that a series of organotin compounds, mainly with biologically active ligands, exhibit promising antitumor

* Corresponding author. Tel./fax: +30 2610 997147.
E-mail address: emane@upatras.gr (E. Manessi-Zoupa).

0162-0134/$ - see front matter © 2008 Elsevier Inc. All rights reserved.
doi:10.1016/j.jinorgbio.2008.01.001

activities [3–7]. From the early studies concerning the potential antitumor activity of organotin compounds, a series of diorganotin derivatives of aminoacids and peptides have been found to exhibit promising antiproliferative activity *in vitro* and *in vivo* [8,9]. The knowledge of specific or selective bonding of organotin species to donor sites in biological structures, and even in simple biologically relevant oligofunctional molecules, is very important for the elucidation of the mechanism of action of these compounds in humans. As peptides can be very effective ligands for a range of metal ions, the study of their interactions with the $R_nSn^{(4-n)+}$ moieties can be one more step to this direction. Despite this, the study of organotin–peptide interactions are still rather scarce [8–10], especially concerning the characterization of the compounds by X-ray crystallography [11–20].

We have initiated [21–23] a systematic study of the coordination chemistry of dipeptides and tripeptides containing the α-aminoisobutyryl residue [–HNC$(CH_3)_2$CO–, Aib]. The α-aminoisobutyric acid (H-Aib-OH, also called α-methyl-alanine or α,α-dimethylglycine) is commonly found in a family of natural antibiotics produced by microbial sources, which are able to alter the ionic permeability of biological membranes by the formation of channels. As shown by early studies, the replacement of the hydrogen atoms of the C_α carbon of glycine with methyl groups produces severe restrictions on the conformational freedom of the molecule and, consequently, Aib is a strong promoter and stabilizer of folded (β-bends) and 3_{10} or α-helical structures [24]. Despite the special properties of Aib, there is a limited number of reports concerning the coordination chemistry of Aib-based small peptides [21–23,25–29]; these reports are confined to copper complexes. Our interest in this chemistry is mainly to investigate how the inductive and steric properties of the α-carbon methyl groups affect the structures of the complexes in the solid state and how this may alter the pharmacological properties of the new compounds.

We wish to report here our chemical and preliminary biological studies concerning the interaction of $(n\text{-Bu})_2Sn^{2+}$ with the dipeptides H-Aib-L-Leu-OH (L_AH) and H-Aib-L-Ala-OH (L_BH) (Chart 1). Emphasis is given on the characterization of the products in the solid state.

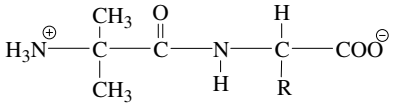

L_AH: R = $CH_2CH(CH_3)_2$

L_BH: R = CH_3

Chart 1.

2. Experimental

2.1. General procedures and physical measurements

All manipulations were performed under aerobic conditions. All chemicals and solvents were purchased from commercial sources and used without further purification. Anhydrous methanol was obtained by distillation. Microanalyses (C, H, N) were performed by the University of Ioannina (Greece) Microanalytical Service using an EA 1108 Carlo Erba analyzer. Tin was determined gravimetrically as tin(IV) dioxide, SnO_2; the samples were decomposed with aqueous ammonia, followed by ignition of the obtained precipitate to stannic oxide. IR spectra (4000–450 cm^{-1}) were recorded on a Perkin–Elmer 16 PC FT spectrometer and a Jasco FT-IR 5300 spectrometers with samples prepared as KBr pellets. Far-IR spectra (500–50 cm^{-1}) were recorded on a Bruker IFS 113v Fourier-transform spectrometer with a liquid nitrogen-cooled MCT detector using polyethylene pellets. FT-Raman data have been collected on a Bruker IFS 66V spectrometer equipped with a FRA 106 Raman accessory, a CW Nd:YAG laser source and a liquid nitrogen-cooled Ge detector. ^{119}Sn NMR spectra for solutions of **1** and **2** in a mixture of $CDCl_3$ and DMSO-d_6 (1:1 v/v) were recorded on a Bruker DRX-300 spectrometer using tetramethyltin(IV) as the internal standard.

2.2. Synthesis of dipeptides

The dipeptides H-Aib-L-Leu-OH (L_AH) and H-Aib-L-Ala-OH were prepared in the liquid phase, as described earlier [22,23].

2.3. Synthesis of complexes

2.3.1. $[(n\text{-}Bu)_2Sn(H_{-1}L_A)] \cdot 2MeOH$ (**1** · 2MeOH)

To a stirred solution of L_AH (0.20 g, 0.93 mmol) in anhydrous methanol (50 ml) was added solid $(n\text{-Bu})_2SnO$ (0.23 g, 0.93 mmol) and the mixture was stirred under reflux. After 30 min all the quantity of the solid dissolved. Stirring under reflux was continued for a further 4 h. The solution, after cooling, was concentrated to a very small volume with a rotary evaporator, yielding a white solid and a colorless oil. Colorless crystals, suitable for crystallographic studies, were obtained by the addition of few drops of anhydrous methanol. Yield: 39%. *Anal.* Calc. for **1**, $C_{18}H_{36}N_2O_3Sn$: C, 48.3; H, 8.1; N, 6.3; Sn, 26.5. Found: C, 48.1; H, 7.9; N, 6.1; Sn, 26.2%.

2.3.2. $[(n\text{-}Bu)_2Sn(H_{-1}L_B)] \cdot MeOH$ (**2** · MeOH)

To a stirred solution of L_BH (0.10 g, 0.57 mmol) in anhydrous methanol (32 ml) was added solid $(n\text{-Bu})_2SnO$ (0.14 g, 0.57 mmol) and the mixture was stirred under reflux. After a few minutes all the quantity of the solid dissolved. Stirring under reflux was continued for a further 2 h. The solution was concentrated to a very small volume

with a rotary evaporator, yielding a colorless oily product. The oil was dissolved in anhydrous MeOH (2 ml). Colorless crystals, suitable for crystallographic studies, were obtained by slow evaporation at room temperature. The crystals were collected by filtration, washed with Et_2O and dried in air. Yield: 41%. *Anal.* Calc. for **2**, $C_{15}H_{30}N_2O_3Sn$: C, 44.5; H, 7.4; N, 6.9; Sn, 29.3. Found: C, 44.2; H, 7.3; N, 6.6; Sn, 29.6%.

2.4. X-ray crystallographic studies

Data collection, crystal data and structure solution information are listed in Table S1 of the Supplementary material. Crystals of complexes **1** · 2MeOH and **2** · MeOH were mounted in capillary. Diffraction measurements were made on a Crystal Logic Dual Goniometer diffractometer using graphite-monochromated Mo radiation. Unit cell dimensions were determined and refined using the angular settings of 25 automatically centered reflections in the range $11° < 2\theta < 23°$. Three standard reflections, monitored every 97 reflections, showed less than 3% variation and no decay. Lorenz, polarization and Ψ-scan absorption corrections were applied using Crystal Logic software.

The structures were solved by direct methods using SHELXS–86 [30] and refined by full-matrix least-squares techniques on F^2 with SHELXL–97 [31]. All hydrogen atoms (except those of the NH_2 group which were located by difference maps and refined isotropically) were introduced at calculated positions as riding on bonded atoms. All non-hydrogen atoms were refined anisotropically.

2.5. Antibacterial activity

The antibacterial activity of the compounds was studied against *Bacillus subtilis* (wild type), *Bacillus cereus* (wild type), *Proteus mirabilis* (wild type) and *Escherichia coli* (XL1). Screening was performed by the method of minimum inhibitory concentration (MIC). The medium of the bacteria growth was LB (Luria–Brettani) [glucose (1.5%, w/v), NaCl 0.5% (w/v), yeast extract 0.5% (w/v) and tryptone 1% (w/v), pH 7.0]. All equipment and culture media were sterile. The compounds were dissolved in DMSO with a 2-fold successive serial dilution from 100 to 3.0 μg/ml. Control cultures in the absence of the studied compounds or in the presence of DMSO were also carried out. All tests were performed in duplicate.

Minimum inhibitory concentration (MIC) is determined using the method of progressive double dilution in liquid media containing 100 to 3.0 μg/ml of the compound being tested. A preculture of bacteria was grown in LB overnight at 37 °C. Four millilitre of LB broth were inoculated with 80 μl of this preculture. This culture was used as control to examine if the growth of the bacteria tested is normal. In a similar second culture 80 μ1 of the bacteria as well as the concentration of the compound tested was added. A third sample containing 4 ml LB supplemented with the same concentration of the compound tested was used as a second control to check the effect of the compound on LB. All samples were in duplicate. We monitored the bacterial growth by measuring the absorbance at 600 nm of the culture in the tubes after 12 and 24 h. If a certain concentration of a compound inhibits bacterial growth we check the effect of the compound at the half concentration. This procedure continues until a concentration in which bacteria grow normally. The latest concentration that inhibits of bacterial growth is the MIC value.

2.6. Effect on pDNA

2.6.1. pDNA isolation

Plasmid pET29c was isolated from *E. coli* XL1 by the alkaline sodium dodecylsulfate (SDS) lysis method (Strategene). All plastics and glassware used in the experiments were autoclaved for 30 min at 120 °C and 130 Kpa.

2.6.2. Agarose gel electrophoresis

One microgram of pDNA were incubated in the presence of the compounds under study in a final volume of 20 μl. The reaction mixture was incubated for 1 h at a constant temperature of 37 °C and terminated by the addition of 5 μl loading buffer consisting of 0.25% bromophenol blue, 0.25% xylene cyanol FF and 30% (v/v) glycerol in water. The products resulting from DNA-compounds interactions were separated by electrophoresis on agarose gels (1.5% w/v), which contained 1 μg/ml ethidium bromide (EtBr) in 40 mM Tris–acetate, pH 7.5, 20 mM sodium acetate, 2 mM Na_2EDTA, at 5 V/cm. Agarose gel electrophoresis was performed in a horizontal gel apparatus (Mini-Sub™ DNA Cell, BioRad) for about 4 h. The gels were visualized in the presence of UV light. All assays were duplicated.

2.7. In vitro cytotoxic activity

2.7.1. Cell lines and culture maintenance

Cell lines used as targets were HeLa (human cervical cancer), HT29 (human colon cancer), OAW-42 (human ovarian cancer) and L929 (normal mouse fibroblasts). All cells were obtained from the Imperial Cancer Research Found (ICRF), London, and the American Tissue Culture Collection (ATCC). Cells were routinely grown as monolayer cell cultures in T-75 flasks (Costar) in an atmosphere containing 5% CO_2 in air and 100% relative humidity at 37 °C and subcultured twice a week, restricting the total number of cell passages below 20. The culture medium used was Dulbecco's modified Eagle's medium (DMEM, Gibco), supplemented with 10% fetal bovine serum (Gibco), 2 mM glutamine (Sigma), 100 μg/ml streptomycin and 100 IU/ml penicillin.

2.7.2. Preparation of the studied agents

All tested compounds were diluted in DMSO. The final concentration of DMSO in the culture was always less than 0.1% w/v, a concentration that produced no effects on cell growth and proliferation, as was experimentally confirmed

(data not shown). A concentrated solution of each agent was prepared in complete growth medium, sterilized via filtration and used to make serial dilutions immediately after the agent was dissolved. Both agents were tested at nine graduated dilutions in the range of 0.1–500 μM.

2.7.3. Trypan blue exclusion

The loss of membrane integrity, as a morphological characteristic for cell death, was assayed by trypan blue exclusion [32]. The number of cells that were alive was estimated through a haematocytometer and phase-contrast microscopy. Each result represented the mean of four independent measurements and used for the inoculation of cells in the microplates.

2.7.4. Cell inoculation – drug exposure – SRB cytotoxicity assay

Cell passages were carried out by detaching adherent, logarithmically growing cells after addition of 2–3 ml of a mixture of 0.05% solution of trypsin (Gibco, 1:250) in phosphate-buffered saline (PBS) with 0.02% EDTA and incubation for 3–5 min at 37 °C. For the experiments, cells were plated (100 μl per well) in 96-well flat-bottom microplates (Costar–Corning) at various cell inoculation densities (Hela and L929: 5000 cells/well, HT29 and OAW-42: 10,000 cells/well) so that untreated cells were in exponential growth phase at the time of cytotoxicity evaluation. Cells were left for 24 h at 37 °C to resume exponential growth and stabilization and afterwards exposed to organotin(IV) complexes for 24 or 48 h by the addition of an equal volume (100 μl) of either complete culture medium (control wells), or twice the final drug concentrations diluted in complete culture medium (test wells). Drug cytotoxicity was measured by means of SRB colorimetric assay estimating the survival fractions (SF) as the percent of control (untreated cells) absorbance. The SRB assay was carried out as previously described [33] and modified by our group [34]. In brief, culture medium was aspirated prior to fixation using a microplate-multiwash device (Tri-Continent Scientific, Inc., Grass Valley, CA) and 50 μl of 10% cold (4 °C) trichloroacetic acid (TCA) were gently added to the wells. Microplates were left for 30 min at 4 °C, washed five times with deionized water and left to dry at room temperature for at least 24 h. Subsequently, 70 μl of 0.4% (w/v) sulforhodamine B (Sigma) in 1% acetic acid solution were added to each well and left at room temperature for 20 min. SRB was removed and the plates were washed five times with 1% acetic acid before air drying. Bound SRB was solubilized with 200 μl of 10 mM unbuffered Tris–base solution and plates were left on a plate shaker for at least 10 min. Absorbance was read in a 96-well plate reader at 492 nm subtracting the background measurement at 620 nm. The test optical density (OD) value was defined as the absorbance of each individual well, minus the blank value (“blank” is the mean optical density of the background control wells, $n = 8$). Mean values and the coefficient of variation (CV) from six replicate wells were calculated automatically. Results were expressed as the “survival fraction” (SF), as shown below.

2.7.5. Calculation of results

For each tested compound a dose–effect curve was produced. Sextuplicate determinations gave a CV (standard deviation/mean%) of much less than 10%, resulting in standard error (SE) which was very low in all cases. The data showing inhibition of cellular growth are expressed as the fraction of cells that remains unaffected (fu) (survival fraction, SF), which is derived from the following equation: fu = ODx/ODc (where ODx and ODc represent the test and the control optical density, respectively). Drug potency was expressed in terms of IC_{50} values (50% inhibitory concentration) calculated from the plotted dose–effect curves (through least-square regression analysis).

3. Results and discussion

3.1. Syntheses

Complexes **1** and **2** were prepared according to the general chemical Eq. (1):

$$(n\text{-Bu})_2\text{SnO} + \text{LH} \xrightarrow[\text{T}]{\text{MeOH}} [(n\text{-Bu})_2\text{Sn}(\text{H}_{-1}\text{L})] + \text{H}_2\text{O} \qquad (1)$$

where $H_{-1}L$ is the doubly deprotonated dipeptide (H-Aib-L-Leu-OH for **1** · 2MeOH and H-Aib-L-Ala-OH for **2** · MeOH).

The above procedure is one of the general methods used for the preparation of organotin(IV) dipeptide complexes [8,9]. All our efforts to isolate complexes of the general formula $[(n\text{-Bu})_2\text{SnL}_2]$, where *L* is the dipeptide monoanion, were unsuccessful, even in the cases where an excess of the ligand or more acidic conditions were used.

3.2. Description of structures

Labeled ORTEP plots of complexes **1** · 2MeOH and **2** · MeOH are shown in Figs. 1 and 2, respectively. Selected interatomic distances and angles are collected in Table 1.

Complex **1** · 2MeOH consists of $[(n\text{-Bu})_2\text{Sn}(\text{H}_{-1}\text{L}_\text{A})]$ units and two lattice MeOH molecules per unit. The Sn^{IV} atom is five-coordinate. The doubly deprotonated dipeptide binds the metal ion *via* the terminal amino nitrogen atom [N(2)], the deprotonated peptide nitrogen atom [N(1)] and one of the carboxylate oxygen atoms [O(1)]. The two remaining coordination sites are occupied by atoms C(11) and C(15) of the two alkyl groups. The five donor atoms within bonding distances define a very distorted polyhedron which is better described as a trigonal bipyramid ($\tau = 0.35$ [35]) with the amino nitrogen and the carboxylate oxygen atoms occupying the axial positions. The great deviation of the O(1)–Sn–N(2) angle [148.7(1) Å] from the ideal value of 180° is probably due to the formation of two chelating rings per ligand $H_{-1}L_A^{2-}$. The metal ion lies only 0.032 Å out of the plane of the equatorial atoms towards N(2), while

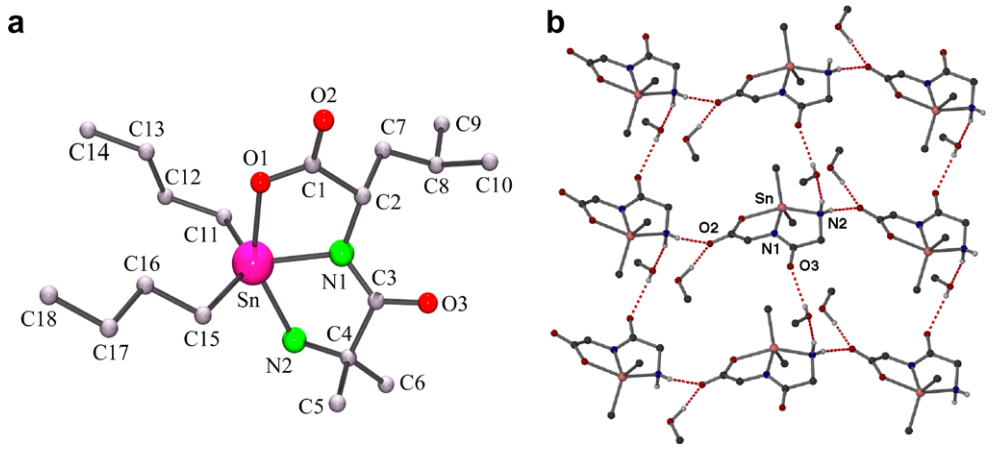

Fig. 1. (a) The molecular structure of complex **1**. (b) The hydrogen-bonded polymeric structure of **1** · 2MeOH; the $[(n\text{-Bu})_2Sn(H_{-1}L_A)]\cdots[(n\text{-Bu})_2Sn(H_{-1}L_A)]$ chains are running parallel to the *b* axis and the 2D network develops parallel to the *ab* plane.

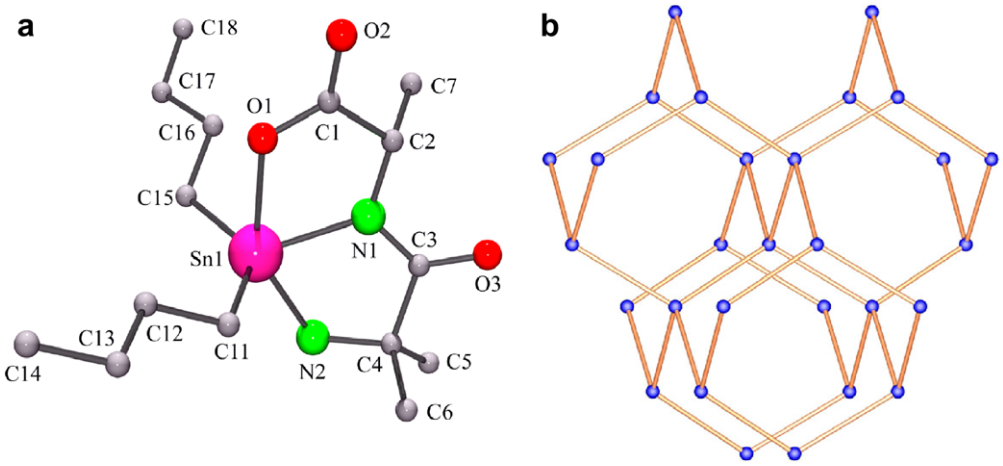

Fig. 2. (a) A partially labelled ORTEP diagram of complex **2**. (b) A schematic representation of the adamantoid network structure of **2** · MeOH.

Table 1
Selected interatomic distances (Å) and angles (°) relevant to the coordination sphere of tin(IV) for complexes **1** · 2MeOH and **2** · MeOH

1 · 2MeOH		**2** · MeOH	
Sn–N(1)	2.107(3)	Sn(1)–N(1)	2.121(4)
Sn–N(2)	2.276(3)	Sn(1)–N(2)	2.235(4)
Sn–O(1)	2.195(2)	Sn(1)–O(1)	2.242(4)
Sn–C(11)	2.138(4)	Sn(1)–C(11)	2.137(5)
Sn–C(15)	2.126(4)	Sn(1)–C(15)	2.130(5)
N(1) –Sn–O(1)	75.5(1)	N(1)–Sn(1)–O(1)	73.8(2)
N(1)–Sn–N(2)	73.6(1)	N(1)–Sn(1)–N(2)	73.8(2)
N(1)–Sn–C(11)	113.7(1)	N(1)–Sn(1)–C(11)	112.6(2)
N(1)–Sn–C(15)	118.4(1)	N(1)–Sn(1)–C(15)	115.4(2)
N(2)–Sn–O(1)	148.7(1)	N(2)–Sn(1)–O(1)	147.6(1)
N(2)–Sn–C(11)	98.7(1)	N(2)–Sn(1)–C(11)	102.8(2)
N(2)–Sn–C(15)	98.0(1)	N(2)–Sn(1)–C(15)	103.9(3)
O(1)–Sn–C(11)	98.3(1)	O(1)–Sn(1)–C(11)	89.8(2)
O(1)–Sn–C(15)	92.0 (1)	O(1)–Sn(1)–C(15)	89.7(2)
C(11)–Sn–C(15)	127.9(2)	C(11)–Sn(1)–C(15)	129.8(2)

the dihedral angle between the two individually almost planar chelating rings SnN(1)C(1)C(2)O(1) and SnN(2)C(4)C(3)N(1) is 18.6°.

In the crystal lattice, a polymeric chain is created by an intermolecular hydrogen bond involving the amine nitrogen [N(2)] and the uncoordinated carboxylate oxygen atom [O(2)] of a neighbouring molecule (Fig. 1b). The chains are connected by intermolecular hydrogen bonds involving the amine nitrogen [N(2)], the methanol oxygen [O(M1)] and the carbonyl oxygen [O(3)] of an adjacent chain, resulting in a 2D hydrogen-bonded framework adopting the (4,4) network structure. The second methanol molecule is hydrogen-bonded to the uncoordinated carboxylate oxygen [O(2)] and does not contribute to the layer formation.

The molecular structure of **2** · MeOH shows a great similarity to that of **1** · 2MeOH and consists of $[(n\text{-Bu})_2Sn(H_{-1}L_B)]$ units and lattice MeOH molecules in an 1:1 ratio.

In the crystal lattice, a polymeric zigzag chain is created by an intermolecular hydrogen bond involving the amine nitrogen atom [N(2)] and one carboxylate oxygen atom [O(1)] of a neighbouring unit. This interaction is supported by a weak contact of the metal ion with the uncoordinated carboxylate oxygen [O(2)] of the same neighbouring unit

[Sn–O(2) $(2-x,\ 0.5+y,\ 0.5-z) = 2.822$ Å]. The chains are connected by intermolecular hydrogen bonds, involving the amine nitrogen[N(2)], the methanol oxygen[O(M1)] and the carbonyl oxygen [O(3)] of an adjacent chain, resulting in a 3D hydrogen-bonded framework adopting a adamantoid network structure. In this arrangement, each [(*n*-Bu)$_2$Sn(H$_{-1}$L$_B$)] acts as a 4-connected node.

Complexes **1** · 2MeOH and **2** · MeOH are members of a small family of Sn(IV)/dipeptide complexes of the general formula [R$_2$Sn(H$_1$L)] which have been characterized by X-ray crystallography [11–20]. Complex **1** · 2MeOH is the second structurally characterized metal complex containing a di- or a monoanionic form of L$_A$H as ligand. The first one is [Cu(H$_{-1}$L$_A$)(MeOH)]$_n$ · *n*MeOH [22], whose structure consists of zigzag polymeric chains; the doubly deprotonated dipeptide behaves as a N(amino), N(peptide), O(carboxylate), O′(carboxylate) μ_2 ligand. Complex **2** · MeOH joins a handful of structurally characterized metal complexes containing any form of L$_B$H as ligand. The two, previously characterized, complexes are [CuClL$_B$]$_n$ · 2.5*n*H$_2$O and [Cu(H$_{-1}$L$_B$)(EtOH)]$_n$ · *n*EtOH [23]. The former is a 3D coordination polymer, in which the dipeptide monoanion L$_B^-$ behaves as an $\eta^1{:}\eta^1{:}\eta^1{:}\mu_2$ ligand binding one Cu^{II} ion through its amino nitrogen and neutral peptide oxygen, and an adjacent Cu^{II} atom through one of its carboxylate oxygens. The latter is a chain (1D) compound, in which the dipeptide dianion H$_{-1}$L$_B^{2-}$ uses its amino nitrogen, deprotonated peptide nitrogen and both carboxylate oxygens to bridge two metal centers. Thus, the coordination modes of H$_{-1}$L$_A^{2-}$ and H$_{-1}$L$_B^{2-}$ observed in **1** · 2MeOH and **2** · MeOH, respectively, are new.

3.3. Spectroscopic properties

Table S2 of the Supplementary material gives detailed assignments of the diagnostic IR bands for the dipeptides L$_A$H, L$_B$H, and complexes **1** and **2**. Assignments have been made by studying extensive literature reports [15,20–23,36–38].

In the spectra of the two complexes we observe the disappearance of the $\nu(NH_3^+)$, $\delta_d(NH_3^+)$ and $\delta_s(NH_3^+)$ bands associated with the zwitterionic configuration of the free dipeptides, and the simultaneous appearance of two absorptions in the 3250–3070 cm^{-1} region assigned [21–23,36] to the antisymmetric and symmetric stretching – NH_2 modes. These changes and the low frequency of the $\nu(NH_2)$ bands are in agreement with the fact that the terminal amino group of H$_{-1}$L$_A^{2-}$ and H$_{-1}$L$_B^{2-}$ occupies one of the coordination sites of Sn^{IV} in the two complexes [21–23]. The differences $\Delta[\Delta = \nu_{as}(CO_2) - \nu_s(CO_2)]$ for complexes **1** (210 cm^{-1}) and **2** (226 cm^{-1}) are larger than the Δ values in the free zwitterionic dipeptides L$_A$H (160 cm^{-1}) and L$_B$H (180 cm^{-1}), respectively, as expected for the monodentate mode of the carboxylate ligation [36,37]. The $\nu_{as}(CO_2)$ and $\nu_s(CO_2)$ vibrational modes in the Raman spectrum of **1** appear at 1607 and 1447 cm^{-1}, respectively [38]; the $\nu_s(CO_2)$ band is very intense, as expected. The corresponding bands in the Raman spectrum of **2** are at 1608 and 1446 cm^{-1}.

The IR and Raman spectra of the free dipeptides L$_A$H and L$_B$H show the characteristic bands of a hydrogen-bonded, *trans* secondary peptide group [38]. As would be expected from the stoichiometry, the IR $\nu(NH)_{peptide}$ band (observed at ~3290 cm^{-1} in L$_A$H and L$_B$H) is absent in the spectra of **1** and **2**. Also the amide II and III bands (due to $[\delta(NH) + \nu(CN)]$ in compounds containing neutral *trans* amide/peptide groups), which appear at ~1550 and ~1250 cm^{-1}, respectively, in the free dipeptides, are replaced by a new strong band at 1368 (**1**) and 1366 (**2**) cm^{-1}, which is characteristic for deprotonated secondary (in fact tertiary) peptide complexes [21–23,38]. This replacement might be expected, since on removal of the peptide proton the band becomes a pure C–N stretch. The $\nu(C{=}O)_{peptide}$ (amide I) band (observed at 1665–1670 cm^{-1} in the free dipeptides L$_A$H and L$_B$H) appears at ~1645 cm^{-1} [coupled with $\delta(NH_2)$] in the spectra of the two complexes; this low-frequency shift is typical of peptide N-bonding [15,20]. The ν(CN) and $\nu(C{=}O)_{peptide}$ modes appear at ~1645 and ~1370 cm^{-1} in the Raman spectra of **1** and **2**.

The two IR bands at ~555 (560 for **1**, 554 for **2**) and ~515 cm^{-1} (517 for **1**, 513 for **2**) are assigned [20] to the $\nu_{as}(SnC_2)$ and $\nu_s(SnC_2)$ modes, respectively. The far-IR spectrum of **1**/**2** exhibit bands at 456/457, 435/430 and 409/410 cm^{-1} assignable to ν(SnN) and ν(SnO) [39].

The ^{119}Sn chemical shift of **1** and **2** in CDCl$_3$/DMSO-d$_6$ are observed at δ −198.1 and −200.7 ppm, respectively. These values are characteristic of five-coordinate di(*n*-butyl)tin(IV) derivatives [40].

3.4. Antibacterial activity

Data on the antibacterial activity of the complexes **1** and **2**, together with those of the starting materials [the dipeptides (L$_A$H, L$_B$H) and (*n*-Bu)$_2$SnO)], against *B. subtilis*, *B. cereus* (gram-positive), *Pr. mirabilis* and *E. coli* (gram-negative) bacteria, are presented in Table 2.

From the MIC values we can conclude that the two ligands and the parent organotin(IV) compound have no activity on the growth of all tested bacteria. Complexes **1** and **2** possessed a significant inhibitory effect against the gram-positive bacteria *B. subtilis* and *B. cereus,* with complex **2** being more active. Since the molecular structures of

Table 2
Antibacterial activity of the tested compounds in MIC (μg ml^{-1})

Compound	Gram-negative bacteria		Gram-positive bacteria	
	E. coli	*P. mirabilis*	*B. subtilis*	*B. cereus*
L$_A$H	>100	>100	>100	>100
L$_B$H	>100	>100	>100	>100
(*n*-Bu)$_2$SnO	>100	>100	100	>100
Complex **1**	>100	>100	25	50
Complex **2**	>100	>100	12	25

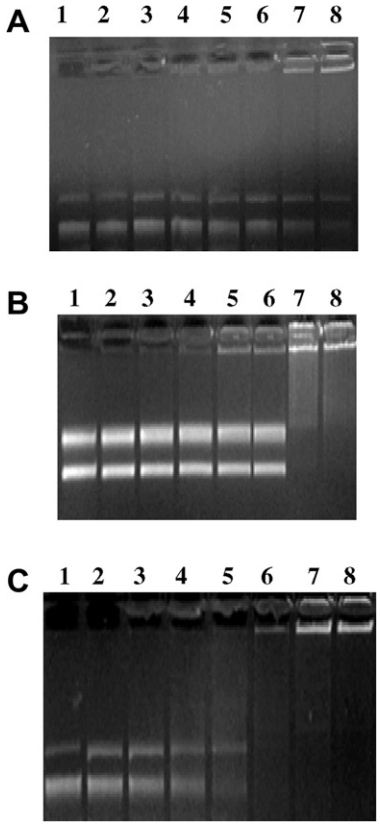

Fig. 3. Agarose gel (1% w/v) electrophoresis of supercoiled and relaxed pDNA (pET29c) incubated with various concentrations of the complexes: (A) Complex **1;** (B) Complex **2;** (C) $(n\text{-Bu})_2SnO$. Each sample contained the same amount of pDNA (1 μg). Lane 1**:** control, plasmid pET29c without treatment. Lanes 2–8**:** plasmid pET29c treated with 0.25, 0.5, 0.75, 1.0, 1.5, 3.0 and 5.0 mM, respectively, of the complex or the starting material.

the two complexes are quite similar, the only difference being the side chain of the second aminoacid of the Aib-containing ligands (–CH_3 in **2** versus –$CH_2CH(CH_3)_2$ in **1**), the above slightly better activity can be attributed to the identity of the second aminoacid of the dipeptide ligand. It was similarly reported that only the gram-positive bacteria are inhibited by other compounds [41], attributed to the fundamental difference in the organisation of their cell wall.

A number of triorganotin(IV)- [10] and diorganotin(IV)-dipeptide [41] complexes have been tested against a panel of gram-positive and gram-negative bacteria. Most of these complexes exhibit promising antibacterial activity, and an attempt has been made for structure–activity relationships [41].

3.5. Effect on pDNA

DNA mobility shift assays were carried out to investigate the ability of the organotin (IV) complexes with dianionic dipeptides, as well as their corresponding free ligands and the starting material (*n*-Bu)SnO to interact with pDNA. The initial amount of pDNA (pET29c, 1 μg), was incubated with increasing concentrations of the tested compounds (Fig. 3). At concentration of complex **1** higher than 3×10^{-3} M (Fig. 3A, lanes 7 and 8) both forms of pET29c (supercoiled and relaxed) were gradually reduced, while a pronounced retardation of the DNA was obtained at the top of the gel. Complex **2** caused a similar effect even at a concentration of 1 mM (Fig. 3B, lanes 5–8). The same experiment was performed with $(n\text{-Bu})_2SnO$ and an up-shift of pDNA was observed for concentrations higher than 1.5 mM (Fig. 3C, lane 6), whereas, the ligands L_BH = H-Aib-L-Ala-OH and L_AH = H-Aib-L-Leu-OH did not display any interaction (data not shown). These results may be assigned to the organotin (IV) interaction with the pDNA. Comparing the crucial concentration of each complex that interacts with DNA, it can be concluded that the incorporation of H-Aib-L-Ala-OH in the organotin(IV) moiety induces better interaction with DNA, compared with that of H-Aib-L-Leu-OH.

3.6. Cytotoxic activity

Cell survival was estimated after 24 or 48 h of exposure to increasing concentrations of complexes **1** and **2**, by means of the SRB assay. To test whether the effect of the Sn(IV) complexes could be attributed to dipeptide ligands alone or not, we tested the effect of these ligands alone

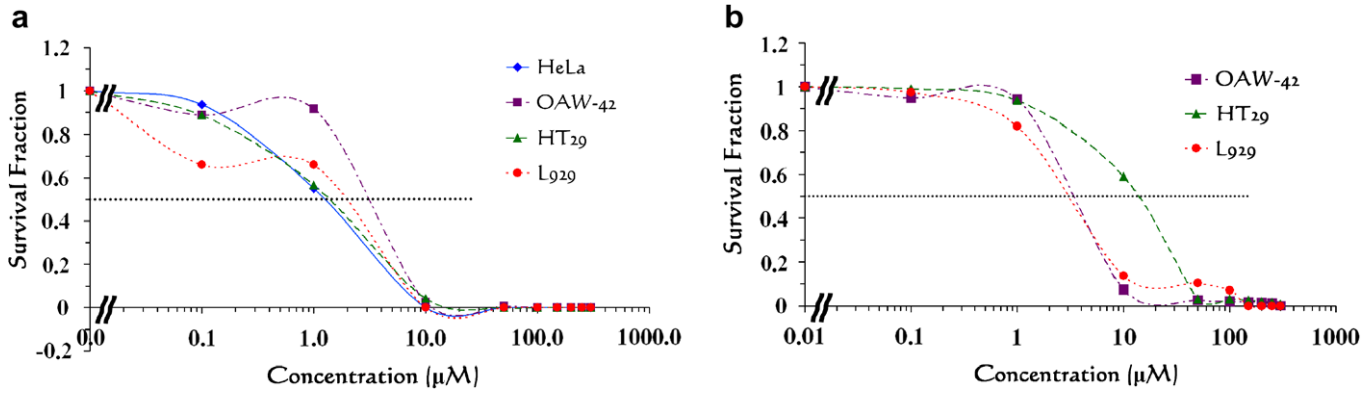

Fig. 4. Dose–effect plots of the complexes **1** (a) and **2** (b) against a panel of human and murine cancer cell lines 48 h (a) or 24 h (b) after the administration of the agents. Cytotoxicity was estimated via SRB assay (each point represents a mean of six replicate wells).

Table 3
IC_{50} values of the tested compounds against HeLa, OAW-42, HT_{29} και L929 cell lines

Compound	IC_{50} (μM)			
	HeLa	HT29	L929	OAW-42
Complex **1**	1.25	1.3	2.0	3.0
Complex **2**	n.d.[a]	13	3.0	3.3
L_AH = H-Aib-L-Ala-OH	>300	>300	>300	>300
L_BH = H-Aib-Leu-OH	>300	>300	>300	>300

[a] n.d. = not done.

against each cell line. The ligands exhibited almost no inhibition of cellular proliferation (data not shown).

Profound growth inhibitory effects were observed for the tested complexes **1** and **2** against a panel of human and murine cancer cell lines. Fig. 4 illustrates the dose–effect plots of various cell lines 24 or 48 h after the administration of complex **1** (a) and **2** (b). The derived IC_{50} values are listed in Table 3.

The *in vitro* cytotoxic activity of the complexes seems rather promising. From the derived IC_{50} values it is concluded that the cytotoxic effect of the organotin(IV)/dipeptide complexes on tested cells was strictly concentration-dependent. OAW-42 and L929 cells revealed to be almost equal in sensitivity against both complexes, while complex **1** found to be more active against HT29 cell line exhibiting a 10-fold lower IC_{50} value compared to complex **2** (1.3 μM vs. 13.0 μM). HeLa cells found to be the most sensitive over the action of **1** with an IC_{50} value of 1.25 μM. Fig. 4 clearly shows the different sensitivity of cell lines to both complexes. The observed sensitivity order revealed to be the following: HeLa > HT29 > L929 > OAW-42 for **1** and L929 > OAW-42 > HT29 for **2**.

Acknowledgements

This work was supported with funds provided by the Research Committee of the University of Patras (C. Karatheodory Programme 2001, No. 2769).

Appendix A. Supplementary data

Crystallographic data (excluding structure factors) in CIF format for the structural analysis have been deposited with the Cambridge Crystallographic Data Centre, CCDC Nos. 645837 (**1**), and 645838. (**2**). Copies of this information may be obtained free of charge from The Director, CCDC, 12 Union Road, Cambridge CB2 1EZ, UK (fax: +44 1223 336 033; e-mail: deposit@ccdc.cam.ac.uk or www:http://www.ccdc.cam.ac.uk) and from the authors upon request. Tables S1 (Crystallographic data for complexes **1** · 2MeOH and **2** · MeOH) and S2 (Most characteristic and diagnostic FT-IR data (cm^{-1}) of L_AH, L_BH and complexes **1** and **2**) are available by the authors upon request. Supplementary data associated with this article can be found, in the online version, at doi:10.1016/j.jinorgbio.2008.01.001.

References

[1] A.J. Crowe, in: M. Gielen (Ed.), Tin-Based Antitumour Drugs, NATO ASI Series H, vol. 37, Springer-Verlag, Heidelberg, 1990, pp. 69–114.
[2] J.M. Tsangaris, D.R. Williams, Appl. Organom. Chem. 6 (1992) 3–18.
[3] A.K. Saxena, F. Huber, Coord. Chem. Rev. 95 (1989) 109–123.
[4] M. Gielen, Coord. Chem. Rev. 151 (1996) 41–51.
[5] L. Tian, Y. Sun, H. Li, X. Zheng, Y. Cheng, X. Liu, B. Qian, J. Inorg. Biochem. 99 (2005) 1646–1652.
[6] D. Kovala-Demertzi, J. Organomet. Chem. 691 (2006) 1767–1774.
[7] C. Pellerito, L. Nagy, L. Pellerito, A. Szorcsik, J. Organomet. Chem. 691 (2006) 1733–1747.
[8] F. Huber, R. Barbieri, in: B.K. Keppler (Ed.), Metal Complexes in Cancer Chemotherapy, VCH, Weinheim, 1993, pp. 353–368.
[9] M. Nath, S. Pokharia, R. Yadav, Coord. Chem. Rev. 215 (2001) 99–149, and references therein.
[10] M. Nath, S. Pokharia, G. Eng, X. Song, A. Kumar, Eur. J. Med. Chem. 40 (2005) 289–298.
[11] F. Huber, H.J. Haupt, H. Preut, R. Barbieri, M.T. Lo Giudice, Z. Anorg. Allg. Chem. 432 (1977) 51–57.
[12] H. Preut, B. Mundus, F. Huber, R. Barbieri, Acta Cryst. C42 (1986) 536–538.
[13] H. Preut, B. Mundus, F. Huber, R. Barbieri, Acta Cryst. C45 (1989) 728–730.
[14] H. Preut, M. Vornefeld, F. Huber, Acta Cryst. C47 (1991) 264–267.
[15] F. Huber, M. Vornefert, H. Preut, E. von Angerer, G. Ruisi, Appl. Organomet. Chem. 6 (1992) 597–606.
[16] B. Mundus-Glowacki, F. Huber, H. Preut, G. Ruisi, R. Barbieri, Appl. Organomet. Chem. 6 (1992) 83–94.
[17] M. Vornefeld, F. Huber, H. Preut, G. Ruisi, R. Barbieri, Appl. Organomet. Chem. 6 (1992) 75–82.
[18] G. Stocco, G. Guli, G. Valle, Acta Cryst. C48 (1992) 2116–2120.
[19] M.A. Girasolo, L. Pellerito, G.C. Stocco, G. Valle, J. Chem. Soc. Dalton Trans. (1996) 1195–1201.
[20] M.A. Girasolo, T. Pizzino, C. Mansueto, G. Valle, G.C. Stocco, Appl. Organomet. Chem. 14 (2000) 197–211.
[21] M. Tiliakos, D. Raptis, A. Terzis, C. Raptopoulou, P. Cordopatis, E. Manessi-Zoupa, Polyhedron 21 (2002) 229–238.
[22] M. Tiliakos, E. Katsoulakou, V. Nastopoulos, A. Terzis, C. Raptopoulou, P. Cordopatis, E. Manessi-Zoupa, J. Inorg. Biochem. 93 (2003) 109–118.
[23] M. Tiliakos, E. Katsoulakou, A. Terzis, C. Raptopoulou, P. Cordopatis, E. Manessi-Zoupa, Inorg. Chem. Commun. 8 (2005) 1085–1089.
[24] E. Benedetti, Biopolymers 40 (1996) 3–44, and references cited therein.
[25] A.W. Hamburg, M.T. Nemeth, D.W. Margerum, Inorg. Chem. 22 (1983) 3535–3541.
[26] L.L. Diaddario, W.R. Robinson, D.W. Margerum, Inorg. Chem. 22 (1983) 1021–1025.
[27] S.T. Kirksey Jr., T.A. Neubecker, D.W. Margerum, J. Am. Chem. Soc. 101 (1979) 1631–1633.
[28] J.P. Hinton, D.W. Margerum, Inorg. Chem. 25 (1986) 3248–3256.
[29] B.E. Schwederski, D.W. Margerum, Inorg. Chem. 28 (1989) 3472–3476.
[30] G.M. Sheldrick, SHELXS-86, Structure Solving Program, University of Göttingen, Germany, 1986.
[31] G.M. Sheldrick, SHELXL-97, Program for the Refinement of Crystal Structures from Diffraction Data, University of Göttingen, Germany, 1997.
[32] A. Gorman, J. McCarthy, D. Finucane, W. Reville, T. Cotter, in: T.G. Cotter, S.J. Martin (Eds.), Techniques in Apoptosis. A User's Guide, Portland Press Ltd, London, UK, 1996, pp. 6–7.

[33] P. Skehan, R. Storeng, D. Scudiero, A. Monks, J. McMahon, D. Vistica, J.T. Warren, H. Bokesch, S. Kenney, M.R. Boyd, J. Natl. Cancer Inst. 82 (1990) 1107–1112.
[34] K.T. Papazisis, G.D. Geromichalos, K.A. Dimitriadis, A.H. Kortsaris, J. Immunol. Methods 208 (1997) 151–158.
[35] A.W. Addison, T.N. Rao, J. Reedijk, J. Rijn, G.C. Verchoor, J. Chem. Soc. Dalton Trans. (1984) 1349–1956.
[36] K. Nakamoto, Infrared and Raman Spectra of Inorganic and Coordination Compounds, fourth ed., Wiley, New York, 1986, pp. 233–244.
[37] G.B. Deacon, R.J. Phillips, Coord. Chem. Rev. 33 (1980) 227–250.
[38] H.O. Desseyn, in: S. Patai (Ed.), The Chemistry of Acid Derivatives, vol. 2, Wiley, New York, 1992, pp. 291–293.
[39] D.M. Adams, Metal–Ligand and Related Vibrations, E. Arnold, London, 1967, pp. 235–315.
[40] M. Nath, S. Pokharia, G. Eng, X. Song, A. Kumar, J. Organomet. Chem. 669 (2003) 109–123.
[41] M. Nath, R. Yadav, G. Eng, T.-T. Nguyen, A. Kumar, J. Organomet. Chem. 577 (1999) 1–8.